Design Sensitivity in Quasi-One-Dimensional Silicon-Based Photonic Crystalline Waveguides

Takeshi Kinoshita, Akira Shimizu, Yukio Iida, and Yasuhisa Omura

Abstract—**This paper describes how the optical properties of a quasi-one-dimensional photonic crystalline waveguide having a periodic air cavity are influenced by various structural parameters; the electromagnetic fields are simulated using the finite-difference time-domain method. The simulations considered four design parameters: cavity size, defect size, lattice constant, and number of cavity. The parameter sensitivity of the photonic bandgap property of the waveguide having air cavities is examined. A couple of significant design guidelines are obtained. We show that the quasi-one-dimensional photonic crystalline waveguide has significant unrealized potential.**

Index Terms—**Quasi-One-Dimensional, Silicon-Based, Waveguides.**

I. INTRODUCTION

The increasing scale of integrated Si devices has given rise to a significant increase in the signal delay time between circuit blocks; the signal delay time is now much longer than the gate delay time of individual devices. It was hoped that this difficulty could be overcome by an advanced metallization technique that replaces Al-based wires with Cu-based wires and the SiO_2-based interlayer dielectrics with a low-k dielectric material. However, it is anticipated that the propagation delay time of interconnections will still determine the speed of integrated circuits when the gate length falls under 0.18 μm. This problem may be overcome by setting optical links between circuit blocks in a chip or LSIs to transfer signals. Silicon-based waveguides have been widely studied from the viewpoints of monolith circuits and process compatibility [1]. The designs must allow for problems such as sharp bends, mode dispersion, and specific attenuation.

Against this background, photonic crystalline (PC) materials are attracting attention for controlling lightwave transmission [2]; photonic bandgap (PBG) structures are especially useful in applications where the spatial localization of lightwaves is required [3]. In a three-dimensional (3-D) PC, we can control the propagation of lightwaves in all directions. Generally speaking, however, it is very difficult to fabricate 3-D PC structures. Its simpler cousin, 1-D PC, offers significant easier fabrication at the cost of reduced functionality. Recently, the influence of defects in 1-D PC waveguides with periodic air cavities has been demonstrated experimentally and the characteristics of such waveguides have been verified by simulations [4]. However, it has not been clarified how design parameters, such as the shape and dimensions of the air cavities, affect the characteristics of the 1-D PC waveguide.

This paper describes how the design parameters of a quasi-1-D PC structure influence its lightwave transmission characteristics. The transmission coefficient is simulated by the finite-difference time-domain (FDTD) method [5] as implemented in a commercial device simulator [6]. Here we assume that the lightwaves have the wavelength (λ) of 1.55 μm because it is representative of modern optical communications systems.

Manuscript received February 13, 2003; revised March 4, 2003.

High-Technology Research Center, Kansai University, 3-3-35, Yamate-cho, Suita, Osaka 564-8680, Japan

II. Device Structure And Simulation Method

We consider a quasi-1-D PC waveguide. The waveguide has a 0.49-μm-wide silicon core (W_{core}) with periodic air cavities and 0.5-μm-thick SiO_2 cladding as shown in Fig. 1, where a is the lattice constant; the figure shows a top view of the waveguide. A break in the periodicity of the air cavities introduces a defect into the quasi-1-D PBG; the defect is allocated in the center of waveguide as shown in Fig. 1. Electromagnetic fields are found by solving Maxwell's equations using the FDTD method. The cell size for computations is $\Delta x=\Delta y=5$ nm.

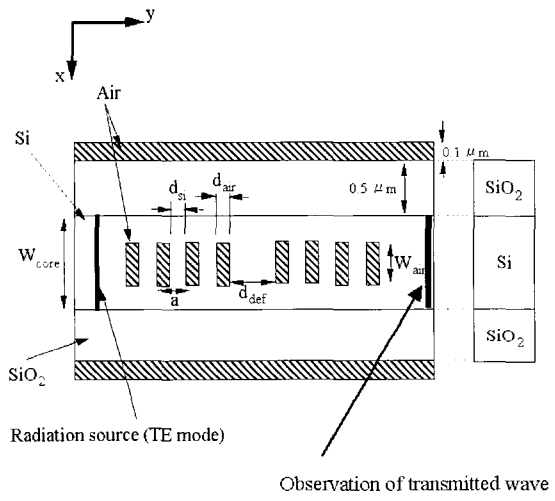

Fig. 1. Waveguide top view. Notations of devices parameters are defined.

Since we carry out 2-D simulations of electromagnetic fields, it is implicit that the waveguide has infinite depth. We use a perfect-matching layer at the computational cell edges. The built-in electromagnetic source radiates a Gaussian-shape wave packet that is modulated over time by a sinusoidal wave; the wave packet has the center frequency of 193 THz. We calculate the transmission coefficient through a waveguide with periodic air cavities; the locations of plane1 (radiation source) and plane2 (observation of transmitted wave) are set appropriately as shown in Fig. 1. Before characterizing the qausi-1-D PC waveguide, we examined the basic propagation property of the waveguide without any air cavities. We found stable lightwave propagation in the frequency range of 90 to 270 THz, which means that a lightwave with λ of 1.55 μm (~200 THz) can transit this waveguide.

III. Simulation Results And Discussion

3.1 *Fundamental parameters for consideration*

In the following discussion, spatial coordinates are normalized by the lattice constant (a) and the angular frequency (ω) is normalized by c/a, where c is the velocity of light in a vacuum. In this sense, the solutions of Maxwell's equations are in themselves independent of the lattice constant, and basically we should be able to discuss PBG characteristics regardless the frequency in the frequency range from microwaves to ultraviolet light. However, the structure shown in Fig. 1 has a silicon core with fixed width (W_{core}), so the lattice constant is still one of the design parameters. Thus, we consider the impact of design parameters (cavity size, defect size, lattice constant, and number of cavities) on PBG characteristics. In addition, we also consider the impact of position deviation of cavity.

3.2 *Influence of air cavity size (W_{air} x d_{air})*

Transmission coefficients were calculated for various values of W_{air} in the range of 30 to 490 nm, while the other design parameters are fixed; a= 300 nm, air cavity spacing (d_{si}) = 120 nm, air cavity length (d_{air}) = 180 nm (d_{si}/d_{air}=2/3), and defect length (d_{def}) = 550 nm. In Fig. 2, simulated transmission coefficients are shown as a function of frequency for the cases of W_{air}= 60, 180, and 360 nm.

As W_{air} increases, the transmission-inhibited band and the frequency of the defect-induced transmission mode shift to a higher frequency range. When W_{air} is designed to range from 120 to 180 nm (W_{air}/W_{core} ranges from 0.245 to 0.367), the transmission coefficient of the transmission-inhibited band has a smaller value than that for W_{air}= 60 or 360 nm. This suggests that there is an optimal value of W_{air} that yields the smallest transmission coefficient.

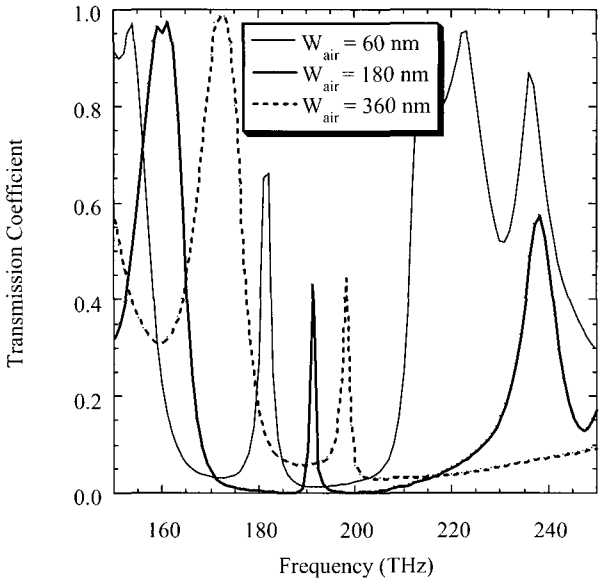

Fig. 2. Transmission coefficient dependence on frequency for various air cavity widths.

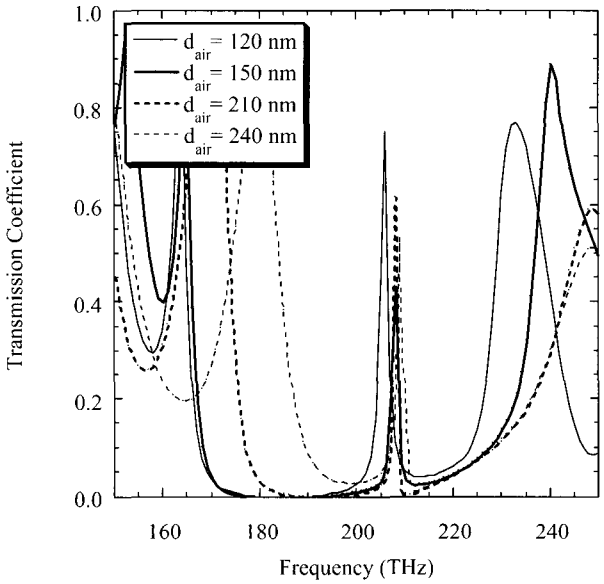

Fig. 3. Transmission coefficient dependence on frequency for various air cavity lengths.

Transmission coefficients were calculated for various values of d_{air}. Simulated transmission coefficients are shown in Fig. 3 as a function of frequency. Since the value of a was fixed, the value of d_{si} was varied automatically. Since the value of d_{air} ranged from 0.1a to 0.9a in simulations, the value of d_{si} ranged from 0.9a to 0.1a. The other design parameters were fixed; a= 300 nm, W_{air} = 180 nm, and d_{def} = 550 nm. In Fig. 3, typical transmission coefficients are shown as a function of frequency in the d_{air} range from 0.4a to 0.8a. As shown in Fig, 3, as the ratio of d_{air} to a increases, the transmission-inhibited band is shifted to a higher frequency range. The frequency of the defect-induced transmission mode also is raised. However, the frequency of the defect-induced transmission mode is quite insensitive to the ratio of d_{air} to a for $0.5a < d_{air} < 0.7a$. For $d_{air} < 0.5a$ or $d_{air} > 0.7a$, transmission coefficients are larger than those for $0.5a < d_{air} < 0.7a$. The transmission coefficient is smallest for d_{air} values from 0.6a to 0.7a.

3.3 *Influence of defect size*

Transmission coefficients were calculated for various values of d_{def}. Simulated transmission coefficient versus frequency is plotted in Fig. 4. The assumed d_{def} values were 470, 520 or 550 nm while the other design parameters were fixed; a= 300 nm, d_{si} = 120 nm, d_{air} = 180 nm (d_{si}/d_{air}=2/3), and W_{air} = 180 nm. As d_{def} increases, the frequency of the defect-induced transmission mode falls while that of the transmission-inhibited band drops only slightly. The bandgap width and the transmission coefficient inside the bandgap are insensitive to d_{def}. A 10-nm variation in d_{def} results in a 2 to 3 THz variation in the frequency of the defect-induced transmission mode (15 to 20 nm in the wavelengh).

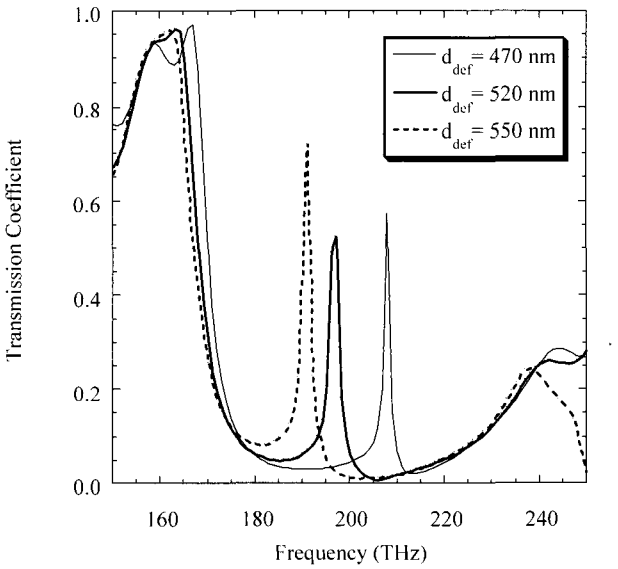

Fig. 4. Transmission coefficient dependence on frequency or various defect lengths.

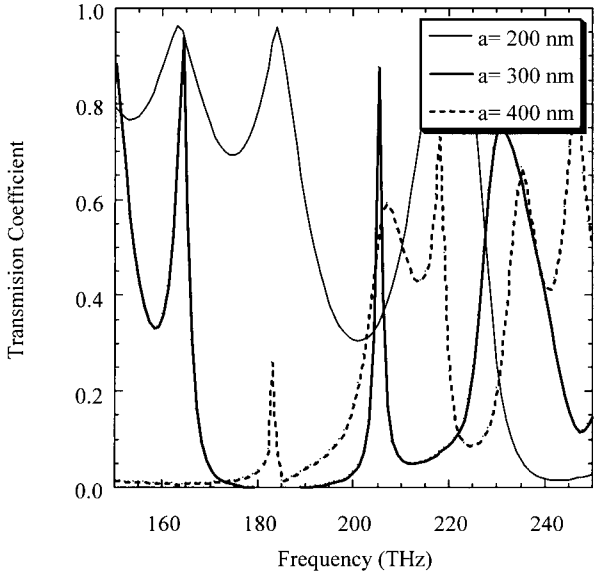

Fig. 5. Transmission coefficient dependence on frequency for various lattice constants.

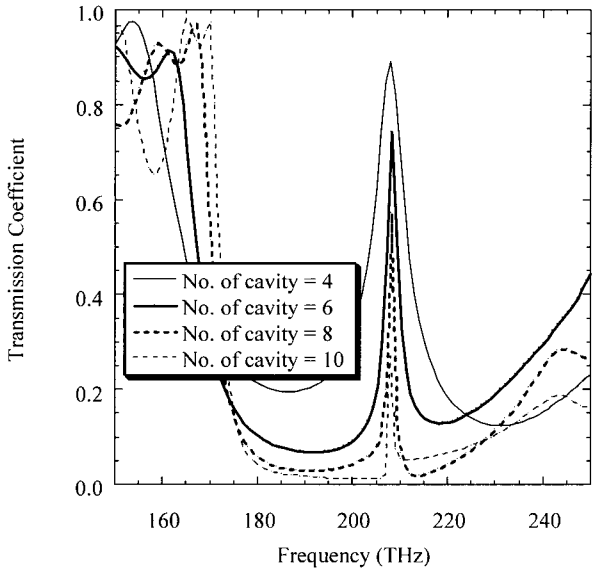

Fig. 6. Transmission coefficient dependence on frequency for various air cavity numbers.

3.4 *Influence of lattice constant*

The frequency dependence of the transmission coefficient was calculated for various lattice constants as shown in Fig. 5. Lattice constant, a, was varied from 200 to 400 nm while the other design parameters were fixed; d_{si} = 0.4a, d_{air} = 0.6a (d_{si}/d_{air}=2/3), and W_{air} = 180 nm. As a increases, the transmission-inhibited band dramatically shifts to a low frequency and the bandgap width increases.

As mentioned in section II, the stable propagation of lightwave is limited to frequencies from 90 to 270 THz. When a = 200 nm, the frequency of the defect-induced transmission mode is higher than 270 THz; the simulation result for a = 200 nm is thus not reliable for the present consideration. The simulation results indicate that the optimal value of a is about 300 nm for W_{core} = 0.5 μm.

3.5 *Effects of number of cavity*

It is known that increasing the number of cavities yields a high quality factor from the analogy of a microwave resonator. Here, we examine how cavity number impacts PBG characteristics. As shown in Fig. 6, transmission coefficients were calculated as a function of frequency for four cavity numbers (4, 6, 8 and 10), while the other design parameters were fixed; a= 300 nm, d_{si} = 120 nm, d_{air} = 180 nm (d_{si}/d_{air}=2/3), W_{air} = 180 nm, and d_{def} = 470 nm. As the cavity number increases, PBG width slightly decreases and the transmission coefficient inside the bandgap decreases.

In this study, the thickness of the Si core is infinite because of the 2-D simulation. For a Si core with finite thickness, the predicted transmission coefficient would be larger than the present simulated value [7].

3.6 *Influence of misalignment of air cavities*

We assumed that the misalignment of air cavities in this waveguide occurred as a structural fluctuation in the fabrication process, and we studied the influence of misalignment of air cavities on photonic bandgap characteristics. We labeled the transverse misalignment of air cavity with M_x and the longitudinal misalignment of air cavity with M_y. Transmission coefficients were calculated for various values of M_x and M_y. Other design parameters were fixed; a = 330 nm, d_{si} = 130 nm, d_{air} = 200 nm (d_{si}/d_{air} = 2/3), W_{air} = 180 nm, d_{def} = 510 nm, and number of cavities is 8. Fundamentally, the waveguide structure designed here is the same as that in the above section, and the frequency of the defect-induced transmission mode is around 193 THz.

Simulated transmission coefficient is shown in Fig. 7

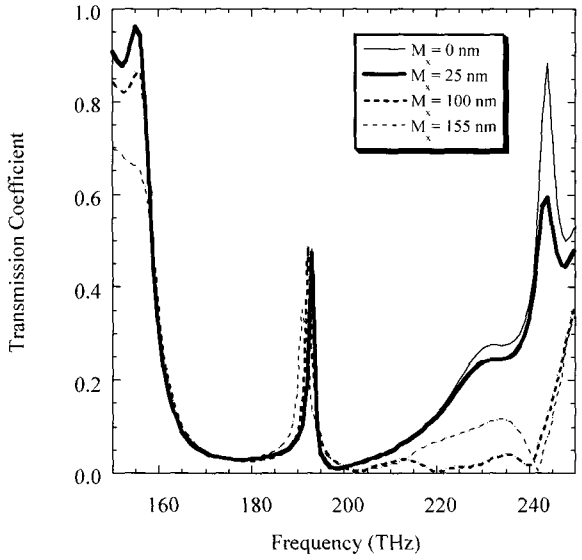

Fig. 7. Transmission coefficient dependence on frequency for various transversal misalignment of air cavity. It is assumed that the location of the third air cavity is shifted in the transverse direction.

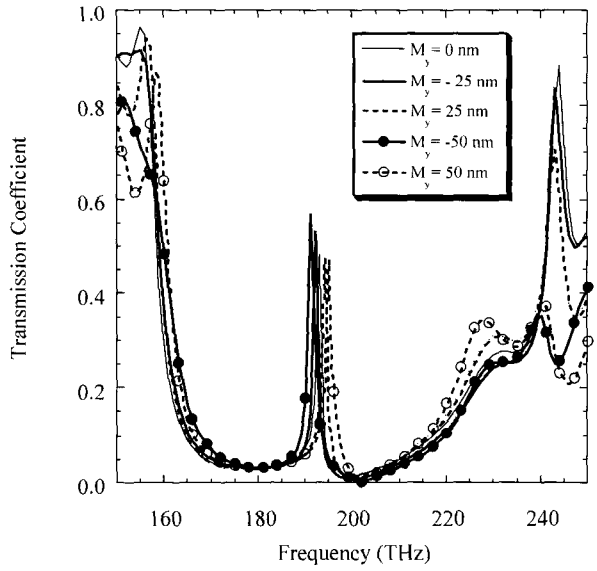

Fig. 8. Transmission coefficient dependence on frequency for various longitudinal misalignment of air cavity. It is assumed that the location of the third air cavity is shifted in the longitudinal direction.

for various M_x values, and here it was assumed that the position of the third air cavity counted from the radiation source side deviated in the transverse direction. M_x is ranging from 25 nm to 155 nm. As M_x increases, the frequency of the defect-induced transmission mode shifts to a low frequency. When the position of the air cavity near the defect location deviates in the transverse direction, the defect-induced transmission mode shifts to a low frequency. The photonic bandgap width and the transmission coefficient inside the bandgap are sensitive to M_x in a high frequency range. When many transversal misalignments of air cavities are found, the total influence of misalignment is given by the sum of influence of each cavity. So, for example, when misalignments of two air cavities are assigned to opposite direction to each other, the influence of misalignment does not finally appear. When M_x is very small, the misalignment of air cavities results in almost no influence on photonic bandgap characteristics.

Transmission coefficient was calculated for various values of a longitudinal misalignment M_y of air cavities. The same design parameters as the above were used; a = 330 nm, d_{si} = 130 nm, d_{air} = 200 nm (d_{si}/d_{air} = 2/3), W_{air} = 180 nm, d_{def} = 510 nm, and number of cavities is 8. Simulated transmission coefficient is shown in Fig. 8 for various values of M_y; My is ranging from –50 nm to + 50 nm. It was also assumed that the position of the third air cavity counted from the radiation source side deviates in the longitudinal direction. When the air cavity gets close to the defect, the defect-induced transmission mode shifts to a high frequency. When the air cavity leaves the defect, the defect-induced transmission mode shifts to a low frequency. This result is similar to that in section 3.3. In other words, influences of the longitudinal misalignment of air cavities correspond to a variation of defect length. However, when M_y is too large (not shown here), then the transmission coefficient of the defect-induced transmission mode is degraded and the width of transmission-inhibited band increases. When there are many longitudinal misalignments of air cavities, the misalignment of air cavity near the defect yields the strongest influence on PBG characteristics. Generally speaking, the influence of longitudinal misalignment of air cavities is notable than that of transversal one because the bandgap structure in qusai-1-D photonic crystal waveguide is based on the mechanism of the Bragg reflection.

IV. Conclusion

We used the FDTD method to simulate the

electromagnetic fields of a quasi-1-D optical waveguide with periodic air cavity. The design parameters considered were cavity size, defect size, lattice constant, and number of cavities. We examined the impact of the parameters on the PBG property of the waveguide.

There is an optimal air cavity width that yields the smallest transmission coefficient. When the ratio of air cavity length (d_{air}) to lattice constant (a) increases, the frequency of the defect-induced transmission mode also increases. However, the frequency of the defect-induced transmission mode is quite insensitive to the ratio of d_{air} to a for $0.5a < d_{air} < 0.7a$. As defect length increases, the frequency of the defect-induced transmission mode falls. PBG width and transmission coefficient inside the PBG are insensitive to defect length. As the cavity number increases, PBG width slightly decreases and the transmission coefficient inside the PBG decreases as expected. It is also demonstrated that transverse or longitudinal misalignment of air cavities near the defect gives rise to a strong influence on PBG characteristics.

These results indicate that characteristics of the quasi-1-D PC waveguide are sensitive to some parameters. However, the design guideline shown here suggests that still it has a bright future since it is easy to fabricate them in comparison to 2-D or 3-D PC waveguides.

ACKNOWLEDGEMENT

This study was financially supported by the Kansai University Research Grants: Grant-in-Aid for Joint Research, 2002.

REFERENCES

[1] R. A. Soref and J. P. Lorenzo, "All-Silicon Active and Passive Guided-Wave Components for =1.3 and 1.6 m," IEEE J. Quantum Electronics, vol. QE-22, no. 6, pp. 873-879 (1986).

[2] E. Yablonovitch, "Inhibited Spontaneous Emission in Solid-State Physics and Electronics," Phys. Rev. Lett., vol. 58, pp. 2059-2062 (1987).

[3] A. Mekis, J. C. Chen, I. Kurland, S. Fan, P. R. Villeneuve, and J. D. Joannopoulos, "High Transmission Through Sharp Bends in Photonic Crystral Waveguides," Phys. Rev. Lett., vol. 77, pp. 3787-3790 (1996).

[4] J. S. Foresi, P. R. Villeneuve, J. Ferrera, E. R. Thoen, G. Steinmeyer, S. Fan, J. D. Joannopoulos, L. C. Kimerling, H. I. Smith and E. P. Ippen, "Photonic-Bandgap Microcavities in Optical Waveguides," Nature, vol. 390, pp. 143-145 (1997).

[5] K. S. Yee, "Numerical Solution of Initial Boundary Value Problem Involving Maxell's Equations in Isotropic Media," IEEE Trans. Antennas Propagat., vol. AP-14, pp. 302-307 (1966).

[6] TCAD "DESSIS and GENESISe" by Integrated Systems Engineering AG. (2001).

[7] P. K. Kelly and M. Piket-May, "Propagation Characteristics for a One-Dimensional Grounded Finite Height Finite Length Electromagnetic Crystal," IEEE J. Lightwave Technol., vol. 17, pp. 2008-2012 (1999).

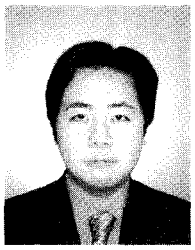

Takeshi Kinoshita was born in1978 in Osaka Pref., Japan, and received the B. S. degrees in Electronics from Kansai University in 2002. He is now a student of graduate school in Kansai University. He is working on the field of physics and design of silicon-based photonic devices.

Mr. Kinoshita is a member of the Japan Society of Applied Physics (JSAP).

Akira Shimizu was born in1978 in Osaka Pref., Japan, and received the B. S. and the M. S. degrees in Electronics from Kansai University in 2000 and 2002, respectively. He is now a student of graduate school in Kansai University. When he was with Kansai University, he was working on the field of physics and design of silicon-based photonic devices and nano-scale devices.

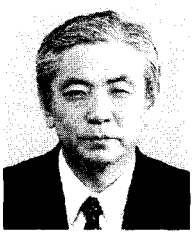

Yukio Iida received the B. E., M. E. and D. Eng. degrees from Kansai University, Osaka, Japan, in 1970, 1972 and 1983, respectively. Since 1979 he has been working at the Department of Electronics, Faculty of Engineering, Kansai University. He was a Research Assistant in 1979, a Lecturer and an Associate Professor. Since 1998 he has been a Professor. He has engaged in the research of microwave electron tube (Osaka-tube and Gyrotron), wireless blasting system by microwave power, injection locking and multiple oscillation in Gunn and IMPATT diodes, injection locking in laser diode, spatial network method, FDTD method, electromagnetic field

simulation, and silicon micro-photonics application including photonic crystal.

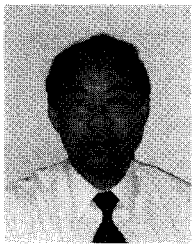

Yasuhisa Omura received the M. S. degree in applied science in 1975 and the Ph. D. degree in electronics in 1984, both from Kyushu University, Japan. He joined the Musashino Electrical Communications Laboratories, NTT, Japan in 1975. He worked on short-channel CMOS/SIMOX design, LSI processing, and SOI device modeling. In NTT, he contributed to trial demonstrations of 1-kb and 4-kb CMOS/SIMOX SRAM on the device design and fabrication processing. He moved his position from NTT Atsugi R&D Center to Kansai University, Osaka Prefecture, as a professor after April in 1997, and he is presently working on device physics of ultimately miniaturized MOSFET/SOI, modeling for MOS device design, physics of transport noise and development of silicon-based photonic devices. He has published 90 regular papers and 66 international conference proceedings. He is one of coauthors having published "Device and Circuit Cryogenic Operation for Low Temperature Electronics." (Kluwer Academic Publishers, 2001)

He served the Technical Committee of IEEE Int. SOI Conf. from 1997 to 1998, and now serves the Program Committee of Int. Symp. on VLSI Technology from 1997 to now. In addition, he serves the Program Committee of European Int. Workshop on Low-Temperature Electronics from 1998.

Dr. Omura is a member of the Japan Society of Applied Physics (JSAP), the Physical Society of Japan, the Electrochemical Society, a senior member of the Institute of Electrical and Electronics Engineers (IEEE) and a member of the Institute of Electronics, Information and Communication Engineers (IEICE).